Available online at www.sciencedirect.com
SCIENCE DIRECT®
Journal of Power Sources 144 (2005) 231–237
JOURNAL OF POWER SOURCES
www.elsevier.com/locate/jpowsour

Room temperature lithium metal batteries based on a new Gel Polymer Electrolyte membrane

L. Sannier[a,*], R. Bouchet[b], S. Grugeon[a], E. Naudin[a], E. Vidal[c], J.-M. Tarascon[a]

[a] *Laboratoire de Réactivité et Chimie des Solides, UPJV, 33 Rue Saint Leu, 80039 Amiens Cedex, France*
[b] *Laboratoire MADIREL, Université de Provence, Centre Saint Jérôme, 13397 Marseille Cedex 20, France*
[c] *EDF, Recherche & Développement, Les Renardières, Route de Sens, 77818 Moret sur Loing Cedex, France*

Received 24 June 2004; received in revised form 24 November 2004; accepted 29 November 2004
Available online 10 February 2005

Abstract

A new effective Gel Polymer Electrolyte membrane based on two polymers, the polyethylene oxide (PEO), a poly(vinylidene fluoride-hexafluoropropylene) (PVdF-HFP) copolymer and a plasticizer, the dibutylphtalate (DBP), was realized. This separator membrane was made by adjunction, through lamination, of an industrially made DBP/PVdF-HFP film and a homemade DBP/PEO thin film. Once the plasticizer was removed and the separator gelled by the electrolyte, the PEO enables the formation of a good interface with the lithium while the PVdF-HFP film brings the mechanical strength to the membrane. The electrochemical behavior of lithium batteries based on this bi-layer separator was investigated versus temperature, cycling potential and cycling rate. Owing to the promising results obtained with laboratory cells, a 1 Ah prototype was successfully assembled, and its cycling and rate performances were reported.

Keywords: Gel Polymer Electrolyte; Lithium batteries; Cycling tests; High capacity prototype

1. Introduction

To face the rapid increase in the portable device market, today's accumulator must sorely improve. While providing great safety benefits, Li-ion batteries are reaching their intrinsic limits in terms of energy and power density. To circumvent such a limitation, possible solution could be the use of metallic lithium systems. Nevertheless, this type of accumulators, well known for ages due to their huge potential, present safety problems associated to the irregular lithium deposition on the lithium metal electrode surface upon subsequent charges, which lead to dendrites formation. Such dendrites enhance the risk of short-circuit, which could promote a thermal runaway of the batteries and, in the worst cases, lead to cell explosion. To circumvent this issue, Armand et al. suggested the use of a dry solid polymer electrolyte consisting of poly(ethylene oxide) (PEO) and a lithium salt [1]. Such an approach, which limits the dendritic growth, comes with the inconvenience of operating the batteries at 60 °C so that the PEO–lithium salt electrolyte membrane can reach sufficient ionic conductivity. In 1994, following a different approach, Bellcore developed a porous polymer membrane mainly based on poly(vinylidene fluoride-co-hexafluoropropylene) (PVdF-HFP) [2]. Once soaked in liquid electrolyte, the polymer is plasticized [3], and the separator presents a high ionic conductivity, a good mechanical strength and no leakage. Nevertheless, even if this system gathers the required qualities to be used as a separator in lithium metal batteries, the polymer composing the membrane does not seem to be stable versus lithium owing to the presence of fluorine atoms [4].

To bypass the above issues, we have combined the advantages of dry and plasticized polymer membranes [5]. More specifically, a PEO film was laminated with a membrane based on PVdF-HFP. Once solvated by the liquid electrolyte,

* Corresponding author. Tel.: +33 3 22827572; fax: +33 3 22827590.
E-mail address: lucas.sannier@sc.u-picardie.fr (L. Sannier).

0378-7753/$ – see front matter © 2005 Elsevier B.V. All rights reserved.
doi:10.1016/j.jpowsour.2004.11.064

the PEO gel ensures a good interface with the lithium, while as in Bellcore technology, the porous PVdF-HFP film brings the mechanical strength to the separator, and acts as a liquid electrolyte reservoir. This kind of membrane, composed of a "soft" buffer between the lithium and a "hard" separator, was termed bi-layer separator, and will be denoted hereafter by the acronym BLS. We had previously studied the intrinsic physical properties of the BLS by means of DSC and X-ray diffraction [6], and found (1) a loss of the PEO crystallinity upon addition of liquid electrolyte into the membrane, (2) an ionic conductivity of the BLS membrane of about 10^{-3} S cm^{-1} similar to the one reported for a Bellcore separator alone [2], (3) a thermal stability of the BLS separator versus lithium metal foil over a wide range of temperatures (−40 °C to 70 °C) by means of impedance spectroscopy, and finally (4) the feasibility of cycling lithium batteries for more than 200 cycles without capacity fading or short-circuits.

Acknowledging these previous findings, this paper focuses on the cycling performance of rechargeable Li/BLS/cathode plastic batteries using cathode materials operating over various potential windows such as $Li_4Ti_5O_{12}$ (mean potential 1.55 V) [7,8] or $LiFePO_4$ (mean potential 3.5 V) [9–13]. Both materials have been intensively studied by several groups because of the positive attributes to fabricate "drugstore" $LiFePO_4/Li_4Ti_5O_{12}$ cells. We found that lithium metal batteries, based on BLS separator, can be cycled over 500 cycles without capacity fading or short-circuits, and demonstrated the possibility of scaling-up our process by realizing a 1 Ah prototype without altering the electrochemical performances.

2. Experimental

2.1. Bi-layer separator preparation

Thirty-five micrometers PVdF-HFP, SiO_2 and dibutylphtalate (DBP)-based membranes were made according to the Bellcore process using a 3/2/4 weight ratio, respectively [14]. PEO thin films were obtained by first mixing in acetonitrile high molecular weight PEO ($M_w = 4 \times 10^6$ g mol^{-1} from Aldrich) and DBP in a 1:1 weight ratio, and then by casting the solution on a Mylar® film using a doctor blade apparatus gapped at 0.15 mm. After room temperature solvent removal, the resulting 10 μm thick film was laminated with a Bellcore PVdF-HFP separator film to form the BLS membrane.

2.2. Composite cathodes preparation

$Li_4Ti_5O_{12}$ material was provided by Telcordia technology, while the $LiFePO_4$ was synthesized and in situ coated by carbon by a method developed in our laboratory [12,13]. Whatever the active material, 2 cm × 2 cm composite cathodes were prepared, outside the glove box, from a mixture of active material (56 wt.%), PVdF-HFP copolymer (15%), DBP (23%) and carbon black (6%) dissolved in acetone. The resulting slurry was spread onto a glass plate resulting in a 50 μm plastic film after solvent evaporation. Within these conditions, a $Li_4Ti_5O_{12}$ composite cathode having 3 mg of active material per cm^2 presents a capacity of about 0.5 mAh cm^{-2}.

2.3. Battery assembly

Cathodes were first laminated together with a pretreated aluminum grid on one side. Then, a second lamination step was performed in order to stick the PVdF-HFP side of the BLS membrane onto the positive electrode. Afterwards, once the DBP extracted by means of several washes into ether solutions, the half-cells were transferred into the glove box, where they were impregnated with a solution of ethylene carbonate–propylene carbonate mixture (EC/PC 1:1 in weight ratio) containing a 1 M dissolved lithium salt $LiN(CF_3SO_2)_2$ (lithium bis(trifluoromethanesulphonyl)imide commercially known as LiTFSI). A lithium foil, pre-laminated on a copper grid, was then placed on top of the cathode/BLS half-cell to produce a battery. In contrast to Bellcore's technology, no lamination step was performed after impregnation of the components because of the capillarity forces created by the PEO/liquid electrolyte gel. Finally, batteries were sealed in hermetic coffee bags, taken out of the glove box, and cycled under different conditions without any external pressure applied.

2.4. Electrochemical measurements

Batteries were cycled at two different temperatures, 20 °C and 55 °C, using a Mac Pile system (Biologic, Claix, France) operating in a galvanostatic mode. Each cell underwent a first slow discharge ($j = -0.2$ mA cm^{-2}) and charge ($j = 0.1$ mA cm^{-2}) to form the active material. This step was followed by a continuous cycling corresponding to a 2-h discharge ($D/2$), and a slow charge ($C/10$) to prevent lithium dendrite formation. For high capacity batteries, a 1-A amplifier was used. Power tests were led by a VMP system (Biologic, Claix, France).

2.5. Cells characterizations

The batteries were cross-sectioned in an argon filled glove box, and placed in a movable airlock system enabling to be put into the scanning electron microscope (SEM) chamber without any air exposure [15,16]. Observations were performed by means of a Philips XL-30 field emission gun SEM.

Accelerating rate calorimetry (ARC) measurements were performed with a calorimeter (Thermal Hazard Technology, Bletchley, England) apparatus to evaluate exothermic runaway processes. The experimental conditions did involve a heating process from 50 °C to 350 °C by steps of 5 °C with a rate of 0.02 °C min^{-1}. After 5 °C heating up, there was a

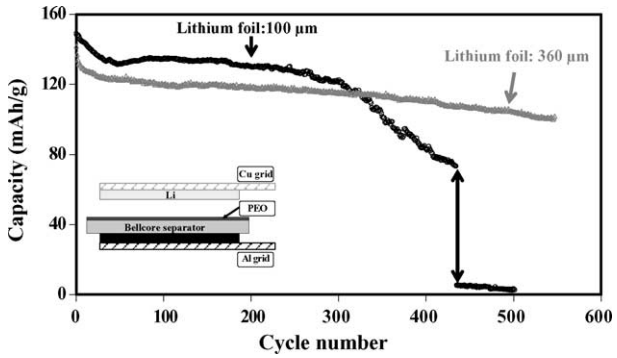

Fig. 1. Cycling test at RT for a BLS lithium battery at *D*/2 (discharge) and *C*/10 (charge) rates using $Li_4Ti_5O_{12}$ as the positive active material and a 100 μm lithium foil (black curve) and a 360 μm lithium foil (grey curve).

rest period (15 min) intended to allow the sample to reach thermal equilibrium.

3. Cycling tests results

Li/BLS/$Li_4Ti_5O_{12}$ batteries were cycled between 1.2 V and 2 V at a *D*/2–*C*/10 rate that corresponds to a current density of $j = -0.25\,mAh\,cm^{-2}$ in discharge and $j = 0.05\,mAh\,cm^{-2}$ in charge (Fig. 1). After a weak initial decrease, the cell capacity remains constant over approximately 300 cycles. Afterward, the capacity continuously decreases, and finally drops down to a few milliamperehours without any evidence for batteries short-circuit. This huge decay was suggested to be rooted in the consumption of all of the lithium. To confirm this hypothesis, cells were assembled with a 360 μm lithium foil instead of 100 μm, and were cycled under similar conditions. No sharp drop in capacity could be observed, strongly indicating that the amount of lithium used as the negative electrode governs the cycling performance of the cell. Cell 1 was cross-sectioned in a glove box, and was then transferred into the SEM chamber by means of a movable airlock system. As shown in Fig. 2, the initial 100 μm lithium foil completely vanishes to the expense of a 300 μm lithium moss that was shown to be electrochemically inactive confirming previous reports [17,18]. Thus, in light of such experimental observations, the decay observed in Fig. 1 could also be interpreted as nested in the growth of a "blocking lithium moss" electrode.

Owing to its high surface area, this irregular lithium deposition was prone to enhance the cell safety hazards. In order to check its reactivity, ARC measurements were performed on an uncycled BLS battery, used as a reference, and a cycled BLS battery containing some lithium moss. Batteries were placed in isotherm conditions for temperatures ranging from 100 °C to 300 °C. For each temperature, the sample temperature increase rate was recorded by a probe in contact with its surface. A peak centered around 180 °C, corresponding to the lithium melt, was detected for both cells (Fig. 3). An additional contribution at 140 °C was observed for the cycled battery, and attributed to the lithium moss presence. However, this peak appears at a temperature quite higher than the security limit required for an industrial production. Furthermore, it is worth noting that the accelerating rate never exceeds $1\,°C\,min^{-1}$. Under this value, the battery could be considered to be in thermal equilibrium with the external environment implying that the lithium moss formation upon cycling does not seem to be too critical in terms of safety.

The same type of battery was prepared by substituting the $Li_4Ti_5O_{12}$ active material for $LiFePO_4$, and using 100 μm lithium foil (Fig. 4). The cell was cycled between 2 V and

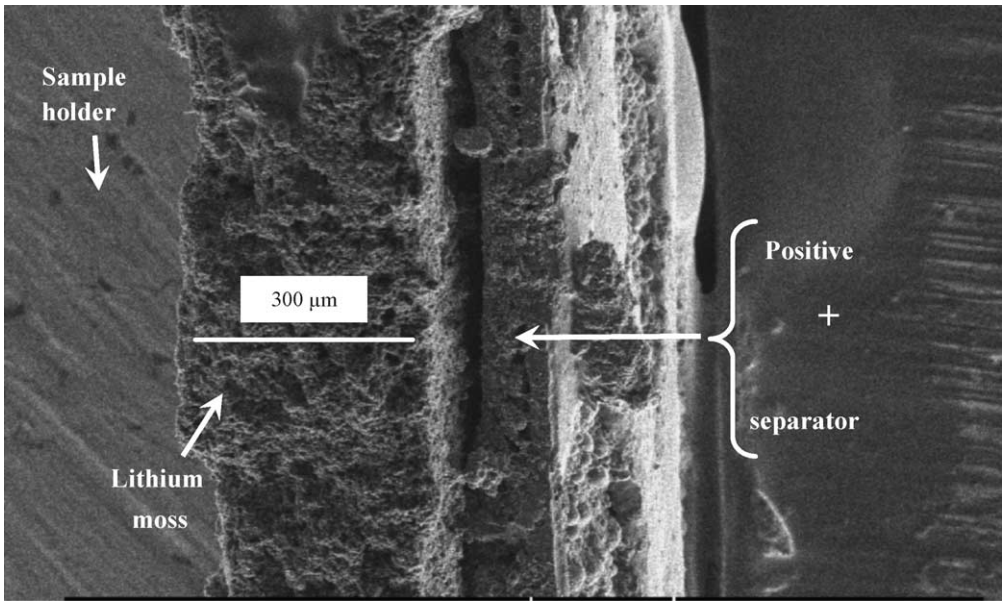

Fig. 2. SEM picture of a cross-section of the battery presented (Fig. 1).

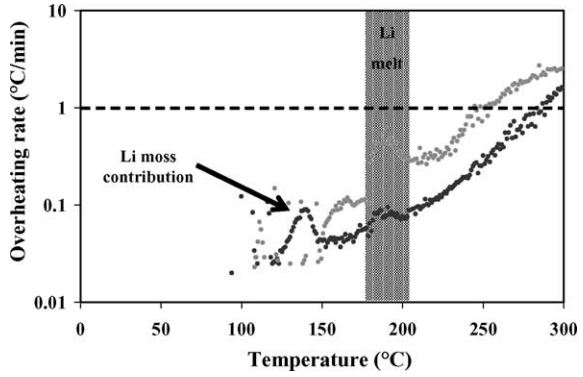

Fig. 3. Accelerating rate calorimetry measurements performed on an uncycled BLS lithium battery (●) and a cycled BLS lithium battery (●).

3.7 V in order to prevent the aluminum collector corrosion induced by the LiTFSI used [19,20]. While using the same lithium foil thickness, but with $LiFePO_4$, instead of $Li_4Ti_5O_{12}$ as cathode, the cell lifetime, in terms of cycling, was at least multiplied by 2, indicating the influence of the active material on the lithium cycling rate. Finally, we should note that cycling tests could be performed with such separator/liquid electrolyte system up to 3.7 V without any interference due to electrolyte or PEO degradation. In short, it appears that the BLS membrane prevents short-circuits from occurring although the lithium deposition is irregular upon cycling. The mossy lithium produced was shown to be unreactive under 140 °C providing a decent temperature range for battery use.

In light of such encouraging results, we embarked in the realization of industrial validation tests. To test self-discharge capabilities, $Li_4Ti_5O_{12}$/BLS/Li batteries were placed in a 55 °C regulated furnace, and stored for weeks. During this time, their potential remained constant meaning that no self-discharge process took place. After each storage period, the cells were discharged and charged at a *D*/2–*C*/10 cycling rate. As reported (Fig. 5), even after 9 weeks of high temperature storage, batteries capacity retention remained unchanged, in good agreement with previous experiments that showed the great thermal stability of the BLS membranes up to 70 °C [6].

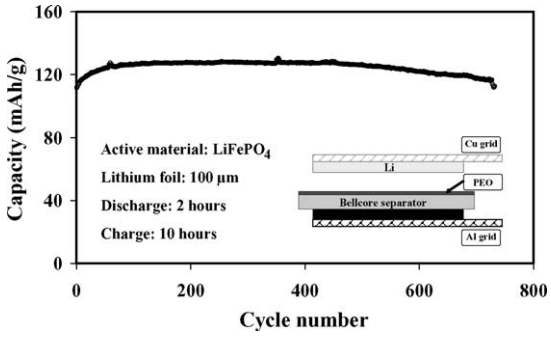

Fig. 4. Cycling test at RT for a BLS lithium battery at *D*/2 (discharge) and *C*/10 (charge) rates using $LiFePO_4$ as the positive active material.

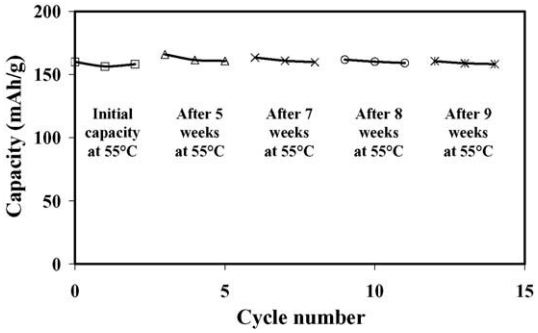

Fig. 5. Evolution of a $Li_4Ti_5O_{12}$/BLS/lithium battery capacity retention stored at 55 °C over weeks.

Similar 55 °C cycling tests at *D*/2–*C*/10 rate were performed on $Li_4Ti_5O_{12}$ cells (Fig. 6). Under these conditions, more than 500 cycles could be achieved before the appearance of a drastic capacity fading as compared to the 300 cycles as previously obtained at room temperature (Fig. 1). Such a difference is most likely nested in the lithium plating/stripping efficiency increase with increasing the temperature [18]. Some experiments are actually in progress in order to check this hypothesis.

Signature tests were also pursued to determine the power rate capacity of $Li_4Ti_5O_{12}$ and $LiFePO_4$ batteries. The test protocol was as follows. The cell was first discharged and charged using low current density, $j = -0.2\,mA\,cm^{-2}$ and $0.1\,mA\,cm^{-2}$, so as to determine the cell nominal capacities, respectively (Fig. 7a). Then, a high rate discharge, corresponding to the use of the whole cell capacity in 30 min (2*D* rate), was applied. Once the limit potential of 2 V reached, the battery was held under open circuit voltage conditions (OCV) during 30 min. The same sequence was repeated several times, dividing the applied current by 2 for each step in order to obtain the Ragone plot presented (Fig. 7b). Power and energy values were expressed as a function of the active material weight. The power rate traces for the two batteries are quite similar to those reported for $LiCoO_2$/C Li-ion batteries, and indicate that all of the cell capacity can be used at a *D* rate. The shift between the Ragone plots for $Li_4Ti_5O_{12}$/Li

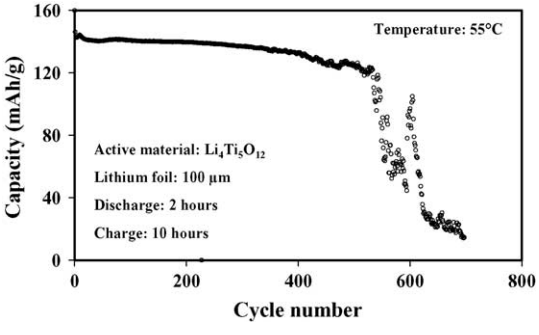

Fig. 6. Cycling test at 55 °C for a BLS lithium battery at *D*/2 (discharge) and *C*/10 (charge) rates using $Li_4Ti_5O_{12}$ as the positive active material and a 100 µm lithium foil.

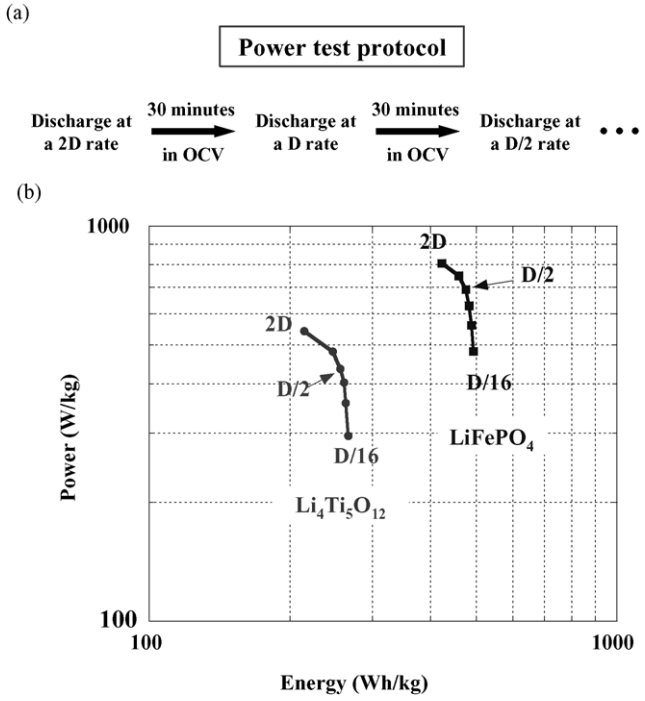

Fig. 7. (a) Description of the power test protocol used and (b) Ragone plot obtained for a $Li_4Ti_5O_{12}$/BLS/lithium battery and a $LiFePO_4$/BLS/lithium battery.

and $LiFePO_4$/Li cells is simply nested in the 2 V difference between their mean redox potentials.

Power rate tests were also performed upon cycling, i.e. every 15 cycles according to the sequence described in Fig. 8a, and as marked with a star in Fig. 8b. Over the 200 first cycles (the maximum we have looked at so far), no capacity decay was observed independently of the power tests performed. Such data suggest that BLS lithium batteries are able to sustain high pulse current density applications while preserving their cycling performance.

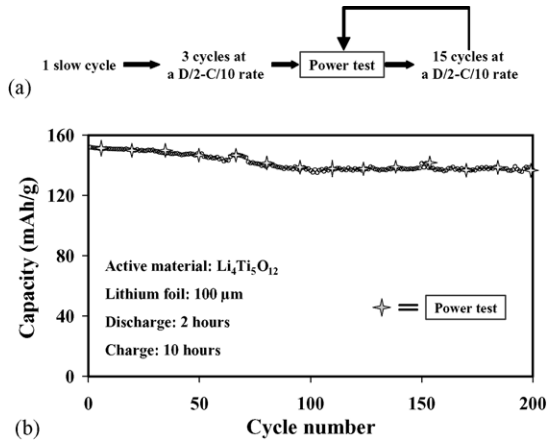

Fig. 8. (a) Description of the alternate cycling/power test protocol used and (b) capacity retention of a $Li_4Ti_5O_{12}$/BLS/lithium battery. (✧) Represents the moment where a power test was performed.

Overall, lithium batteries based on BLS membranes appear to present all of the required qualities in terms of cyclability, self-discharge, temperature stability and high current density acceptance, thus our incentive to implement such a separator concept to the assembly of 1 Ah capacity prototype cells.

4. Large size prototypes

The $Li_4Ti_5O_{12}$/BLS/Li 1 Ah battery configuration, which consists in several cells in parallel, has been inspired from the supercapacitor prototype developed by Bellcore [21] (Fig. 9a). To reach the required capacity, eight 60 mm × 150 mm tapes of composite electrode (e.g. overall cathode surface of 720 cm^2) were placed in front of the lithium metal electrode on a packed together final battery stacking that, once activated by adding electrolyte, was sealed into a hermetic coffee bag so as to produce a 100 mm × 230 mm battery (Fig. 9b). The assembled cell was discharged and charged at a low current density of $j = -0.2$ mA cm^{-2} and 0.1 mA cm^{-2}, for about six cycles, respectively (Fig. 10). Nevertheless, the large capacity of 1 Ah was reached, owing to the thickness of the composite positive electrodes close to 150 μm, our prototypes did present an important polarization reaching 250 mV even at this low cycling rate.

To overcome this polarization issue, positive electrodes thickness was divided by almost 3 while maintaining the surface area constant so that the prototype theoretical capacity was slightly lower than 400 mAh. As before, the cell was cycled at low current drains for the first 22 cycles (Fig. 11). With a thinner positive electrode, no capacity decay was observed.

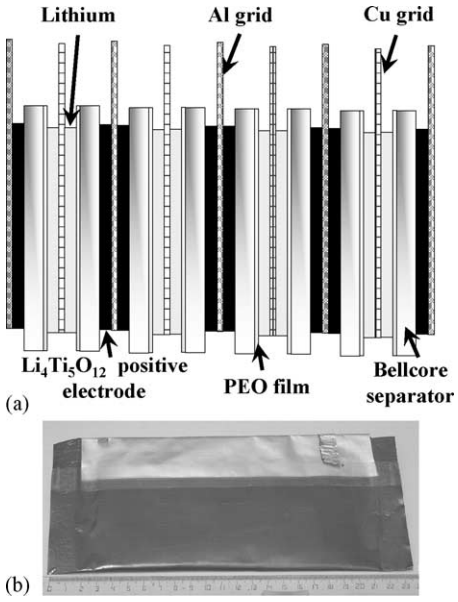

Fig. 9. (a) Schematic representation of the 1 Ah $Li_4Ti_5O_{12}$/BLS/lithium battery configuration and (b) picture of the 1 Ah battery.

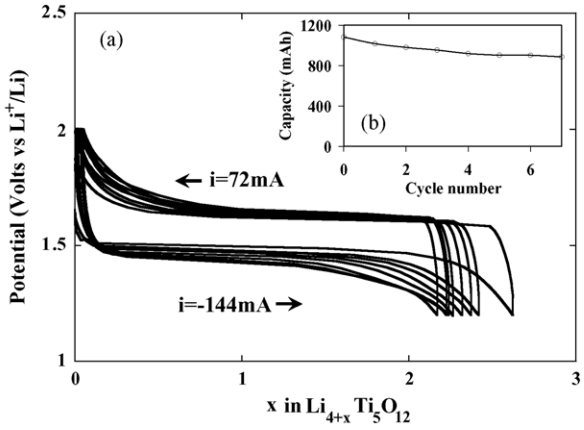

Fig. 10. (a) Composition vs. potential curve and (b) capacity retention of the first seven cycles of the 1 Ah $Li_4Ti_5O_{12}$/BLS/lithium battery.

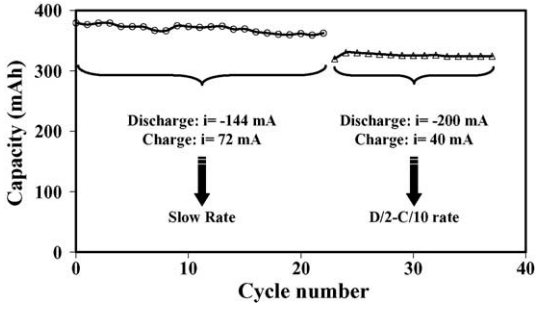

Fig. 11. Capacity retention of a 400 mAh $Li_4Ti_5O_{12}$/BLS/lithium battery.

Note that increasing the current density to reach a *D*/2–*C*/10 rate did not affect the cell capacity retention at least for the first 15 cycles we tried. Finally, we experienced that by thinning the electrode to 50 μm, the polarization value dropped to 100 mV.

Overall, besides the polarization issues, the realization of high capacity laboratory prototypes clearly conveys the easy scalability of BLS-based lithium batteries, since the 1 Ah cell behaves as the 2 mAh laboratory specimens. Needless to say that numerous improvements could be industrially performed in the prototype assembly, as we are presently doing, in conjunction with a battery manufacturer.

5. Conclusions

We have shown different experiments confirming the positive attributes of a bi-layered PEO/PVdF-HFP separator. Based on this membrane design, plastic batteries, having a capacity ranging from 2 mAh to 1 Ah, were assembled and cycled at a *D*/2–*C*/10 rate without any short-circuit evidence. The cycling lifetime of such cells was shown to be solely governed by the excess amount of lithium used as negative electrode. Upon cycling, irregularly plated during the battery charge, part of the lithium was becoming electrochemically inactive and forming a moss. The reactivity of this "dead lithium" was investigated by ARC measurements, which did not reveal any accident until a temperature of 140 °C, providing them a safe margin as compared to the (−20 °C; 70 °C) temperature domain, in which these batteries are supposed to be used. In addition, while presenting decent rate capabilities together with the feasibility of being used under pulse application, BLS lithium batteries do not present a self-discharge or capacity fading process even after a long stay at 55 °C.

Nevertheless, the loss of active lithium over cycling stands as the main problem. Investigations are in progress to improve the lithium deposition efficiency, and therefore, battery attractiveness with respect to energy density and cycling retention. The benefit that such a system could present over Li ion cells is presently cancelled by the fact that we must operate in large excess of lithium (e.g. decreasing the overall cell energy density).

Acknowledgements

The authors are indebted to both the French Agency for Environment and Energy organization (ADEME) and the French Ministry of Research under a national team effort program named ALEP, for their strong support of this work. We are also thankful to C. Wurm for providing the $LiFePO_4$ material used to assemble plastic cells and S. Lascaud for fruitful discussions considering safety aspects.

References

[1] M. Armand, J.M. Chabagno, M.J. Duclot, in: P. Vashista, J.N. Mundy, G.K. Shenoy (Eds.), Fast Transport in Solids, North-Holland, New York, 1979, p. 131.
[2] J.-M. Tarascon, A.S. Gozdz, C. Schmutz, F. Shokoohi, P.C. Warren, Solid State Ionics 86–88 (1) (1996) 49.
[3] J.-M. Tarascon, M. Armand, Nat. Lond. 414 (6861) (2001) 359.
[4] H.S. Choe, J. Giaccai, M. Alamgir, K.M. Abraham, Electrochim. Acta 40 (13–14) (1995) 2289.
[5] L. Sannier, S. Grugeon, S. Lascaud, J.-M. Tarascon, Accumulateur au lithium avec separateur bi ou tri couches, FR0207433 (2002).
[6] L. Sannier, R. Bouchet, L. Santinacci, S. Grugeon, J.-M. Tarascon, J. Electrochem. Soc. 151 (6) (2004) A873.
[7] L. Kavan, M. Gratzel, Electrochem. Solid State Lett. 5 (2) (2002) A39.
[8] K. Zaghib, M. Simoneau, M. Armand, M. Gauthier, J. Power Sources 81–82 (1999) 300.
[9] A.K. Padhi, K.S. Nanjundaswamy, J.B. Goodenough, J. Electrochem. Soc. 144 (4) (1997) 1188.
[10] A.K. Padhi, K.S. Nanjundaswamy, C. Masquelier, S. Okada, J.B. Goodenough, J. Electrochem. Soc. 144 (5) (1997) 1609.
[11] N. Ravet, Y. Chouinard, J.F. Magnan, S. Besner, M. Gauthier, M. Armand, J. Power Sources 97–98 (2001) 503.
[12] A. Audemer, C. Wurm, M. Morcrette, S. Gwizdala, C. Masquelier, Carbon-caoted Li-containing powders and process for production thereof, WO 2004/001881 A2 (2003).

[13] C. Wurm, M. Morcrette, S. Gwizdala, C. Masquelier, Lithium transition-metal phosphate powder for rechargeable batteries, US 2004/0175614 Al (2004).
[14] A.S. Gozdz, C. Schmutz, J.-M. Tarascon, Rechargeable lithium intercalation battery with hybrid polymeric electrolyte, US 5296318 (1994).
[15] F. Orsini, A. Du Pasquier, B. Beaudoin, J.M. Tarascon, M. Trentin, N. Langenhuizen, B.E. de, P. Notten, J. Power Sources 76 (1) (1998) 19.
[16] M. Dolle, L. Sannier, B. Beaudoin, M. Trentin, J.M. Tarascon, Electrochem. Solid State Lett. 5 (12) (2002) A286.
[17] P.C. Howlett, D.R. MacFarlane, A.F. Hollenkamp, J. Power Sources 114 (2003) 277.
[18] H. Ota, X.M. Wang, E. Yasukawa, J. Electrochem. Soc. 151 (2004) A427.
[19] W. Xianming, E. Yasukawa, S. Mori, Electrochim. Acta 45 (17) (2000) 2677.
[20] Y. Haesik, K. Kyungjung, T.M. Devine, J.W. Evans, J. Electrochem. Soc. 147 (12) (2000) 4399.
[21] G. Amatucci, A. Du Pasquier, J.-M. Tarascon, Supercapacitor structure, US 6181545 (2001).